Spatio-temporal dynamics of charge transport in LGAD probed with focused ion beams

41st RD50 workshop – Sevilla, Spain

November 29th – December 2nd, 2022

Andreo Crnjac[1], Milko Jakšić[1], Mauricio Rodriguez-Ramos[1,*], Gregor Kramberger[2]

[1] Laboratory for Ion Beam Interactions, Ruđer Bošković Institute, Zagreb, Croatia
[2] Jožef Stefan Institute, Ljubljana, Slovenia
[*] *Present address:* Centro Nacional de Aceleradores, Universidad de Sevilla, Sevilla, Spain

Ruđer Bošković Institute

Overview

Ion microprobe

- MeV ions – heavy ionizing particles
- Charge transport probing with IBIC

Gain suppression in LGAD

- Control of ionization density by:
  - Different ion M/E
  - Change of the angle of incidence
- KDetSim modelling of lateral diffusion during charge collection

Additional examples

- Ion-TCT signal analysis for LGADS
- Rad. damage studies

Overview

AT SPATIAL AND TEMPORAL SCALES RELEVANT FOR OBSERVING THE UNDERLAYING SOLID-STATE DYNAMICS

Ion microprobe

- MeV ions – heavy ionizing particles
- Charge transport probing with IBIC

Gain suppression in LGAD

- Control of ionization density by:
  - Different ion M/E
  - Change of the angle of incidence
- KDetSim modelling of lateral diffusion during charge collection

Additional examples

- Ion-TCT signal analysis for LGADS
- Rad. damage studies

Ion microbeam – semiconductor charge transport probing

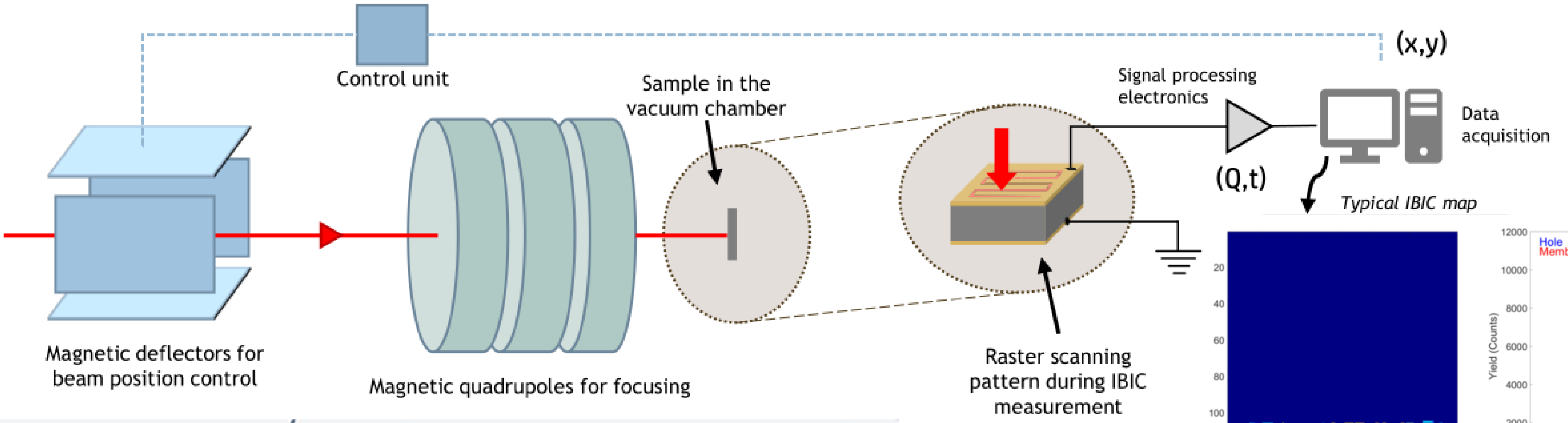

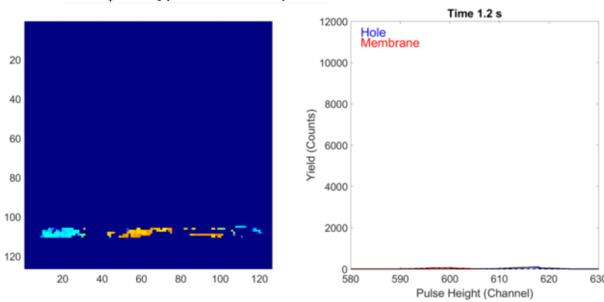

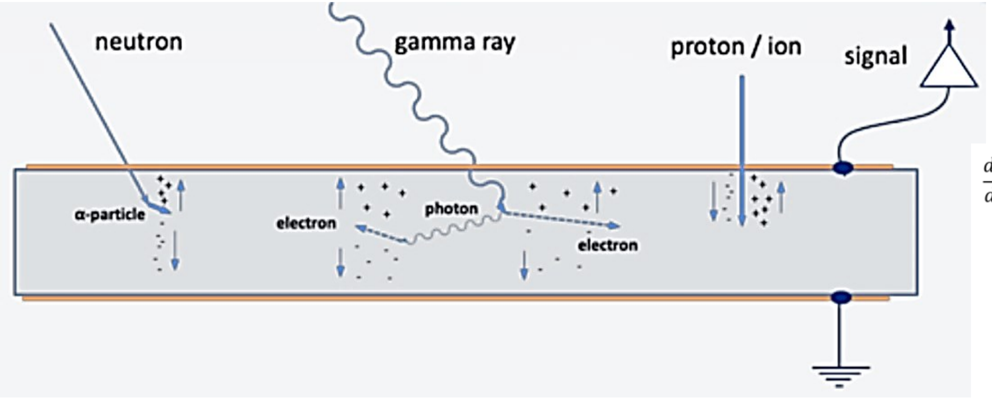

IN THIS STUDY:

$$\frac{\mathbf{d}E}{\mathbf{d}x}\ \mathbf{100 - 12000}\ MeV/cm$$

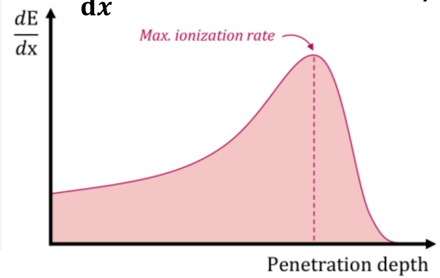

- Spatial mapping
- Depth probing and ionization density
- Ion rate control

Charge transport in LGAD using **IBIC** technique

- **Ion Beam Induced Charge** microscopy

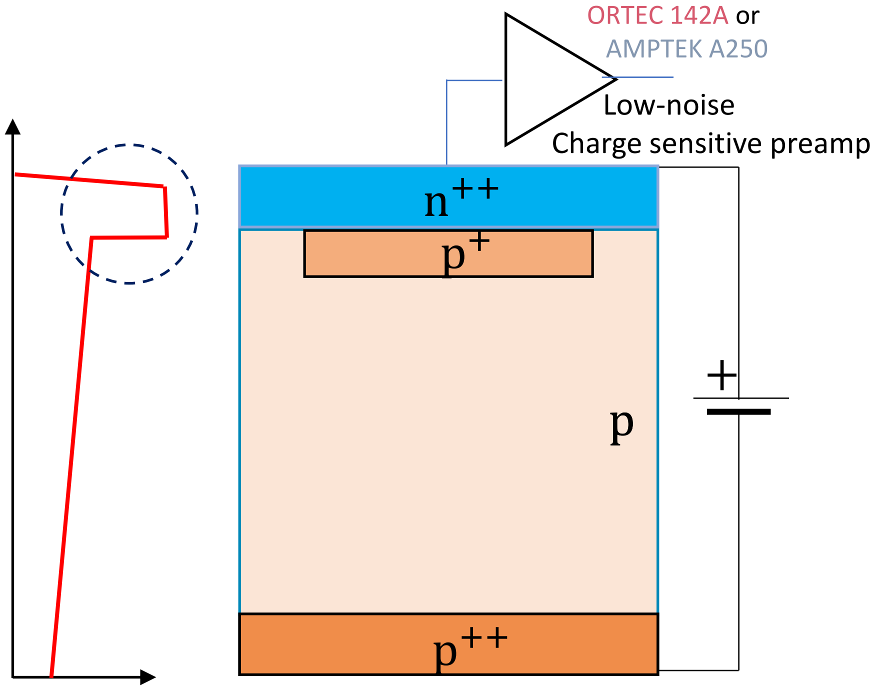

LGAD samples info:

Active volume: 50 µm

Full depletion: 61 V

Breakdown: ≈160 V

$N_{eff}\ (\mathrm{p}^{+}) \sim (e^{16} - e^{17})cm^{-3}$

$N_{eff}\ (\mathrm{n}^{++}) \sim e^{20}cm^{-3}$

$N_{eff}\ (\mathrm{p}^{+}) \sim (e^{16} - e^{17})cm^{-3}$

Charge transport in LGAD using **IBIC** technique

- **Ion Beam Induced Charge** microscopy

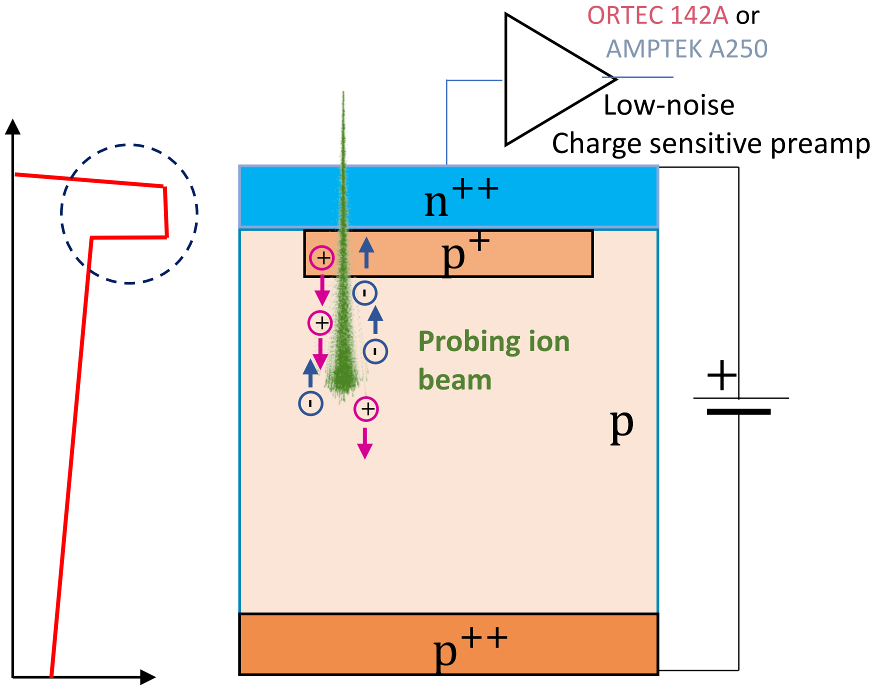

LGAD samples info:

Active volume: 50 µm

Full depletion: 61 V

Breakdown: ≈160 V

$N_{eff}\ (\mathrm{p}^{+}) \sim (e^{16} - e^{17})cm^{-3}$

$N_{eff}\ (\mathrm{n}^{++}) \sim e^{20}cm^{-3}$

$N_{eff}\ (\mathrm{p}^{+}) \sim (e^{16} - e^{17})cm^{-3}$

Charge transport in LGAD using **IBIC** technique

- **Ion Beam Induced Charge** microscopy

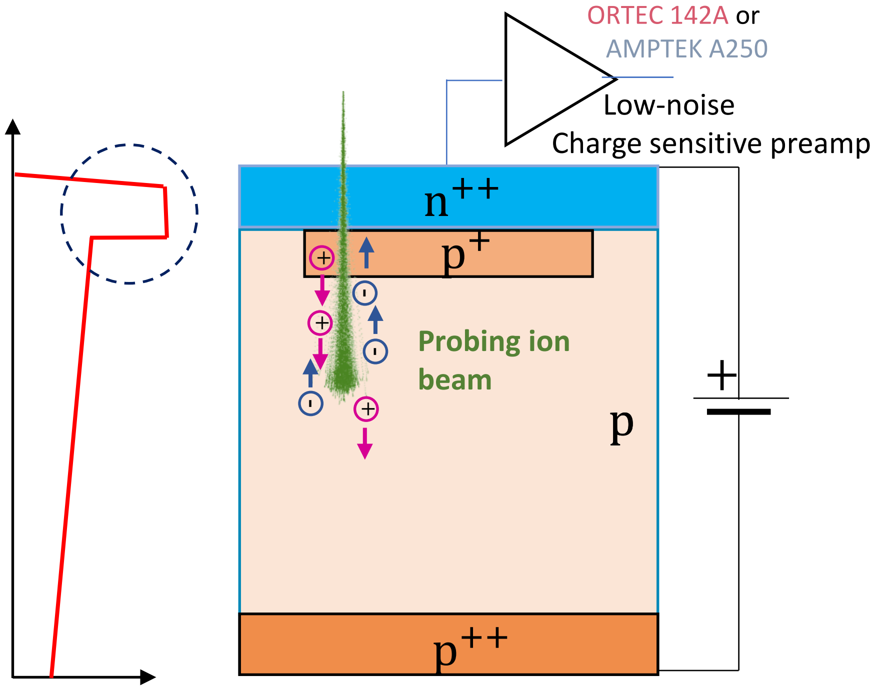

Interaction volume between the ion and the detector is well defined

Spatially resolved information

LGAD samples info:

Active volume: 50 µm

Full depletion: 61 V

Breakdown: ≈160 V

$N_{eff}\ (\mathrm{p}^{+}) \sim (e^{16} - e^{17})cm^{-3}$

$N_{eff}\ (\mathrm{n}^{++}) \sim e^{20}cm^{-3}$

$N_{eff}\ (\mathrm{p}^{+}) \sim (e^{16} - e^{17})cm^{-3}$

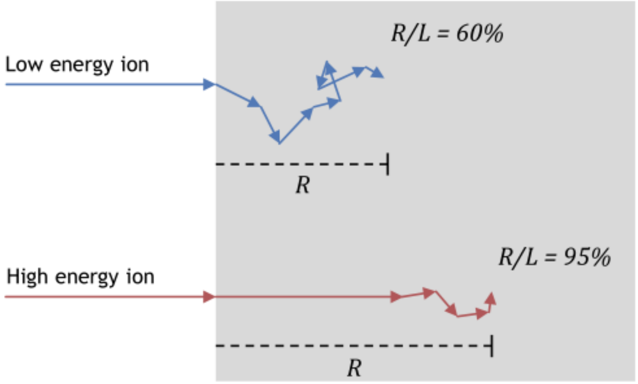

Charge transport in LGAD using **IBIC** technique

- **Ion Beam Induced Charge** microscopy

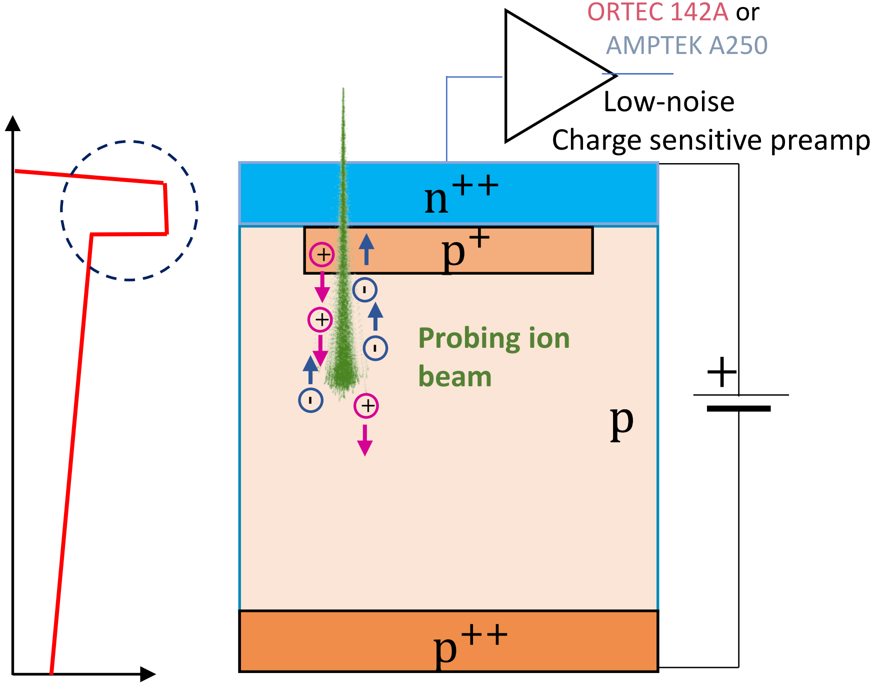

Interaction volume between the ion and the detector is well defined

Spatially resolved information

LGAD samples info:

Active volume: 50 µm

Full depletion: 61 V

Breakdown: ≈160 V

$N_{eff}\ (\mathrm{p}^{+}) \sim (e^{16} - e^{17})cm^{-3}$

$N_{eff}\ (\mathrm{n}^{++}) \sim e^{20}cm^{-3}$

$N_{eff}\ (\mathrm{p}^{+}) \sim (e^{16} - e^{17})cm^{-3}$

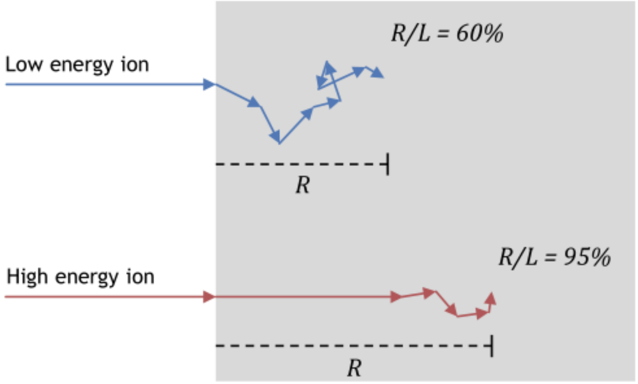

Spatial resolution defined by the beam spot, usually **≤ 1 µm**

Charge transport in LGAD using **IBIC** technique

- **Ion Beam Induced Charge** microscopy

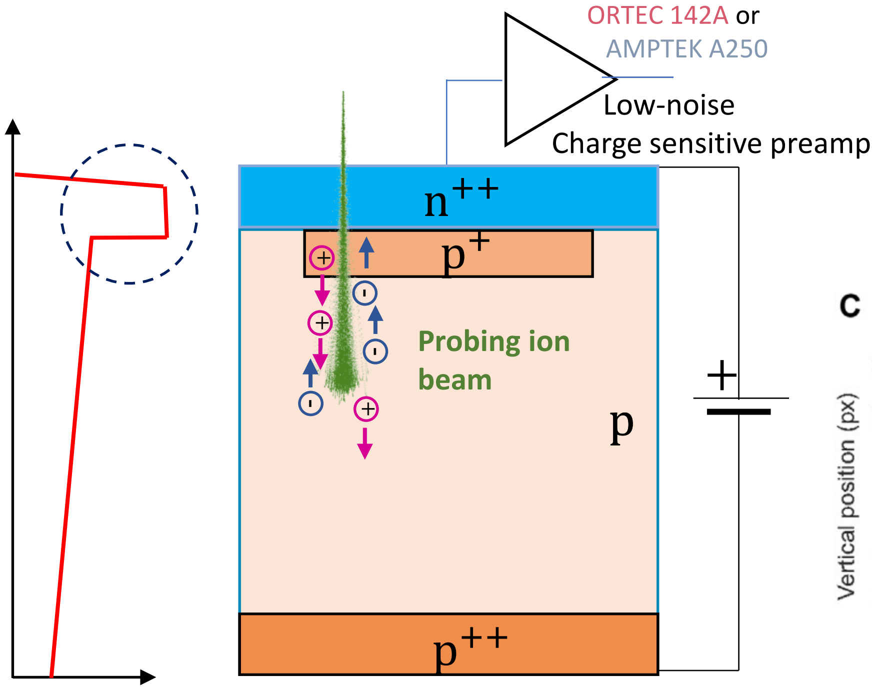

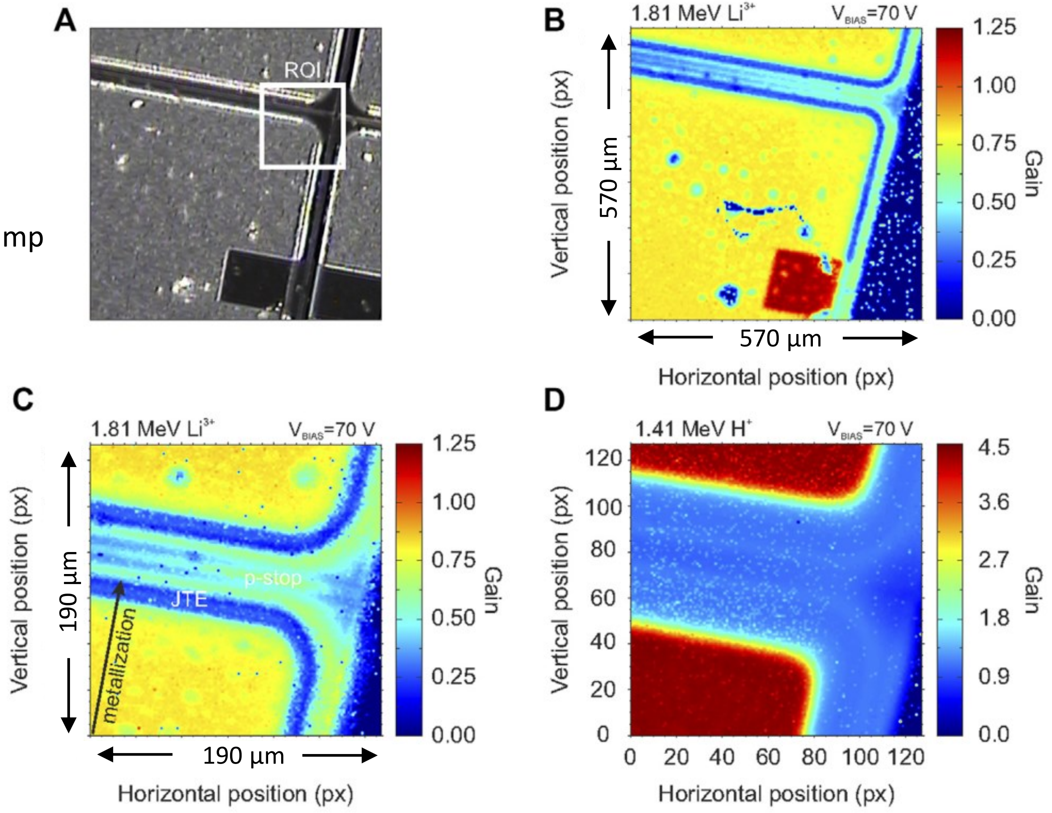

Spatial resolution defined by the beam spot, usually **≤ 1 µm**

Gain suppression in Low Gain Avalanche Diodes (LGAD)

Lower then expected signal amplitude has been observed in studies with **MeV ions, laser light and alpha particles** [REF: 1, 2]

Results published in May 22 [Ref: 3]

Our goal: investigate the role of *ionization density* using MeV ions with

1) different penetration depths,

2) changing angle of incidence

Gain suppression in Low Gain Avalanche Diodes (LGAD)

Lower then expected signal amplitude has been observed in studies with **MeV ions, laser light and alpha particles** [REF: 1, 2]

Results published in May 22 [Ref: 3]

Our goal: investigate the role of *ionization density* using MeV ions with

1) different penetration depths,

2) changing angle of incidence

1) Different penetration depths

Gain suppression in Low Gain Avalanche Diodes (LGAD)

Lower then expected signal amplitude has been observed in studies with **MeV ions, laser light and alpha particles** [REF: 1, 2]

Results published in May 22 [Ref: 3]

Our goal: investigate the role of *ionization density* using MeV ions with

1) different penetration depths,

2) changing angle of incidence

1) Different penetration depths

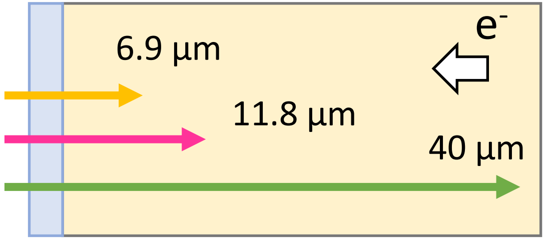

3 proton energies

Max. ionization at different depths

For **deep protons** -> peak gain at FDV

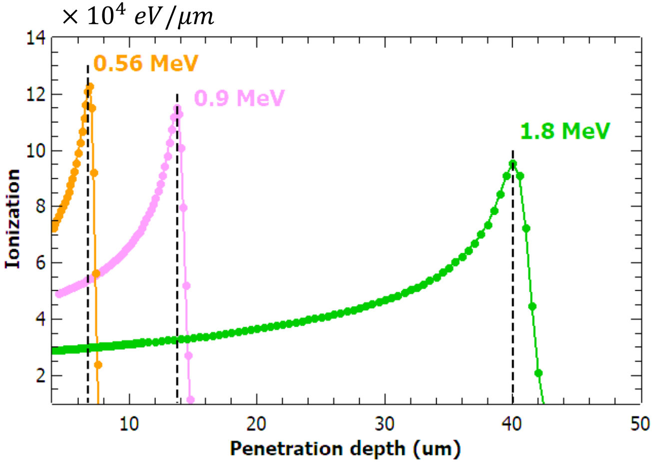

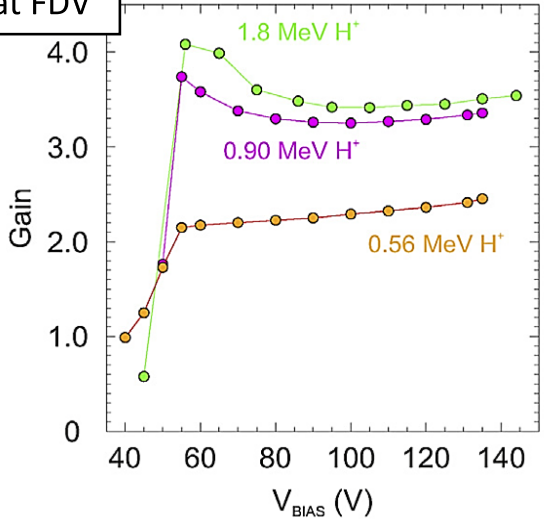

Gain suppression in Low Gain Avalanche Diodes (LGAD)

1) Different penetration depths

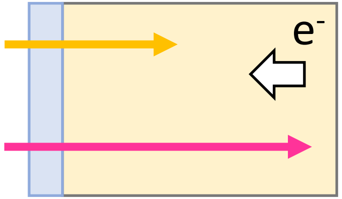

2) Changing angle of incidence

Gain suppression in Low Gain Avalanche Diodes (LGAD)

1) Different penetration depths

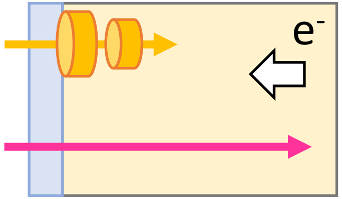

2) Changing angle of incidence

Gain suppression in Low Gain Avalanche Diodes (LGAD)

1) Different penetration depths

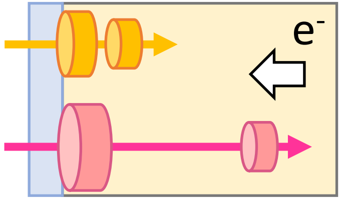

2) Changing angle of incidence

Gain suppression in Low Gain Avalanche Diodes (LGAD)

1) Different penetration depths

Higher el. field
-> faster drift

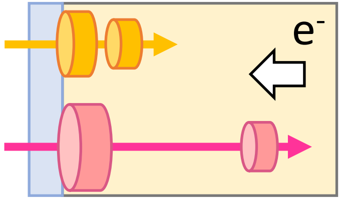

G. Kramberger – KDetSim code

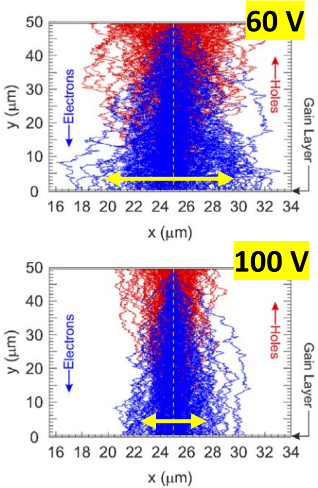

2) Changing angle of incidence

Gain suppression in Low Gain Avalanche Diodes (LGAD)

1) Different penetration depths

Higher el. field
-> faster drift

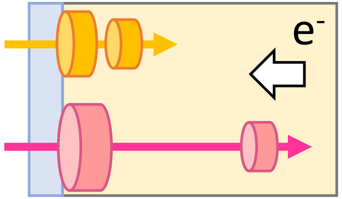

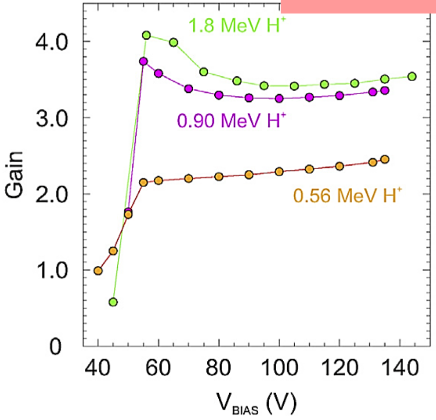

G. Kramberger – KDetSim code

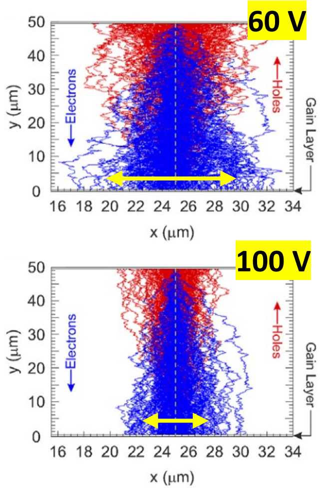

2) Changing angle of incidence

Gain suppression in Low Gain Avalanche Diodes (LGAD)

1) Different penetration depths

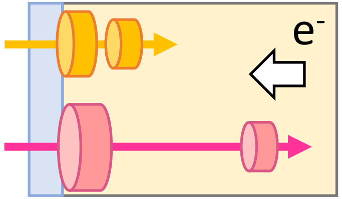

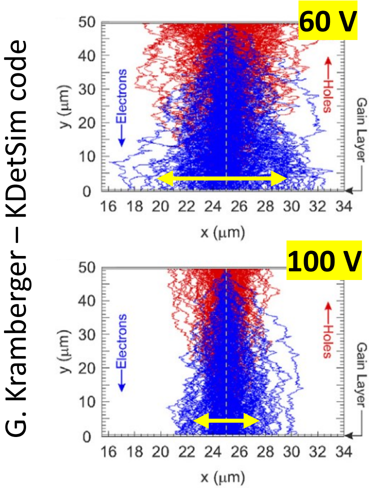

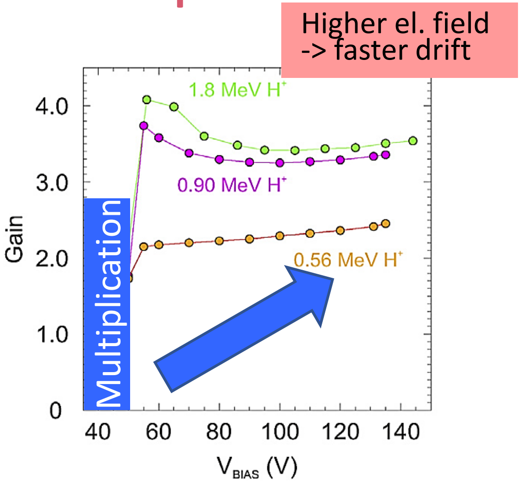

2) Changing angle of incidence

Gain suppression in Low Gain Avalanche Diodes (LGAD)

1) Different penetration depths

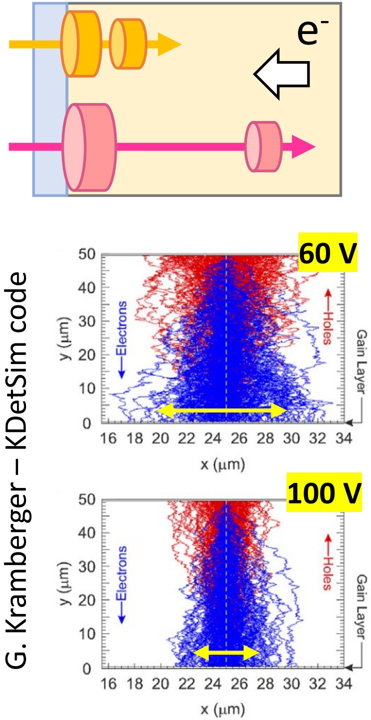

G. Kramberger – KDetSim code

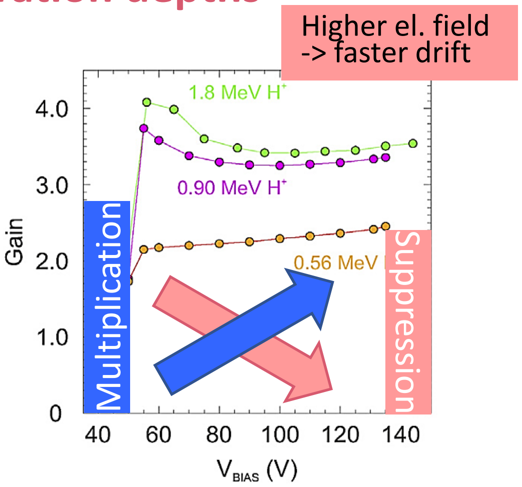

Increased electric field **screening** at higher bias due to the faster drift and smaller lateral spread of the charge cloud (diffusion)

2) Changing angle of incidence

Gain suppression in Low Gain Avalanche Diodes (LGAD)

1) Different penetration depths

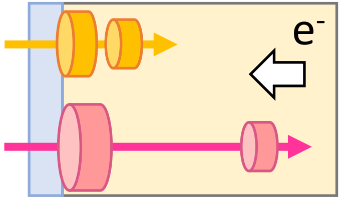

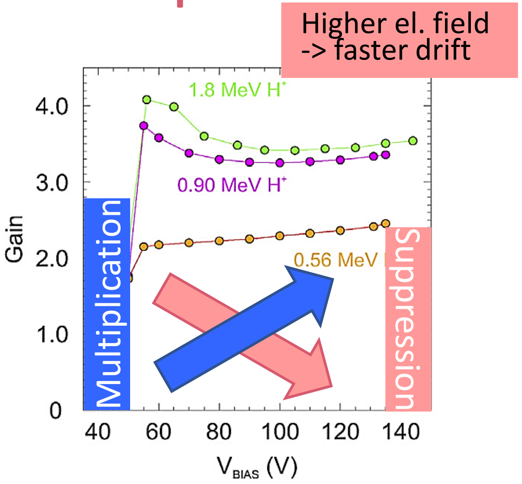

G. Kramberger – KDetSim code

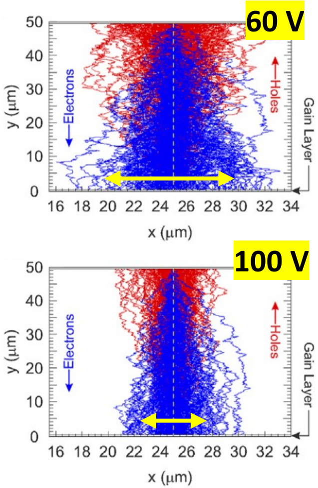

Increased electric field **screening** at higher bias due to the faster drift and smaller lateral spread of the charge cloud (diffusion)

2) Changing angle of incidence

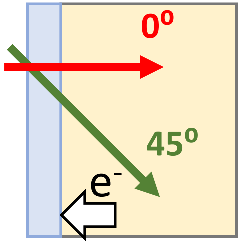

Gain suppression in Low Gain Avalanche Diodes (LGAD)

1) Different penetration depths

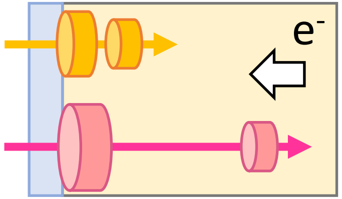

G. Kramberger – KDetSim code

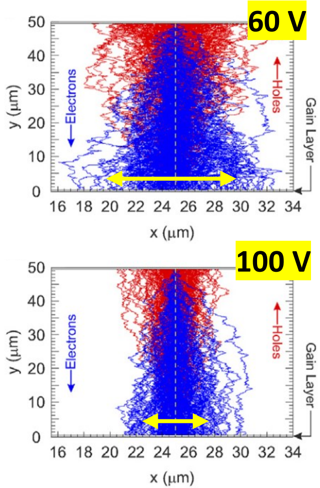

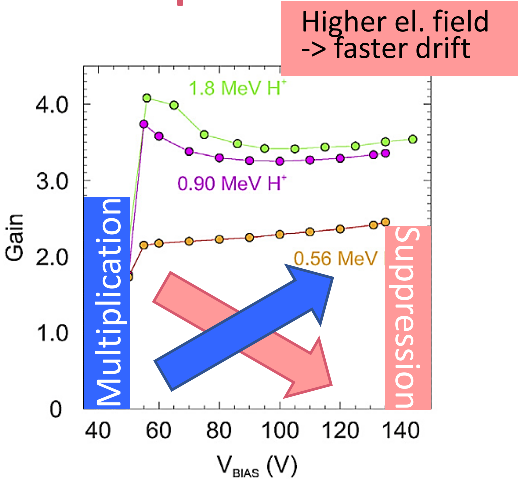

Increased electric field **screening** at higher bias due to the faster drift and smaller lateral spread of the charge cloud (diffusion)

2) Changing angle of incidence

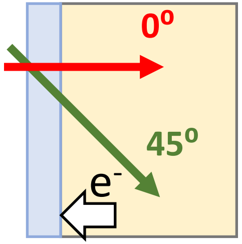

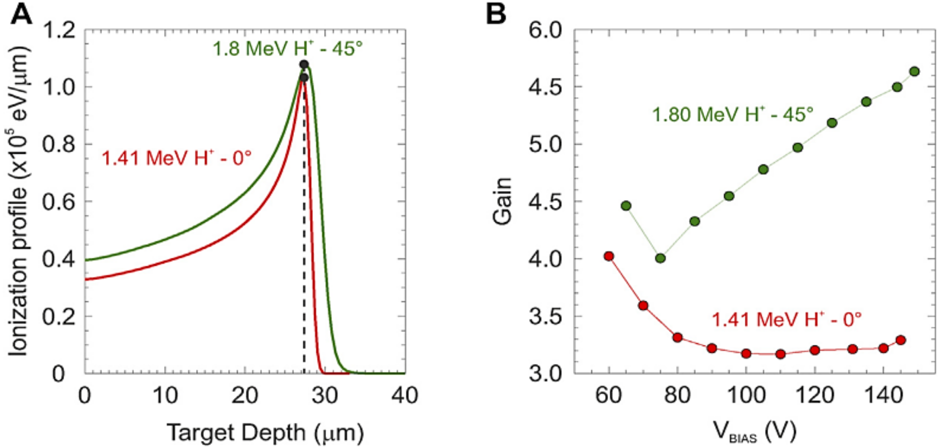

Gain suppression in Low Gain Avalanche Diodes (LGAD)

1) Different penetration depths

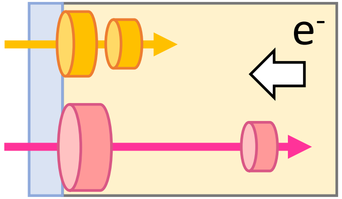

Higher el. field
-> faster drift

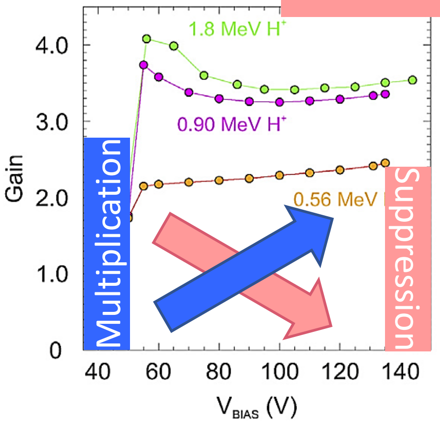

G. Kramberger – KDetSim code

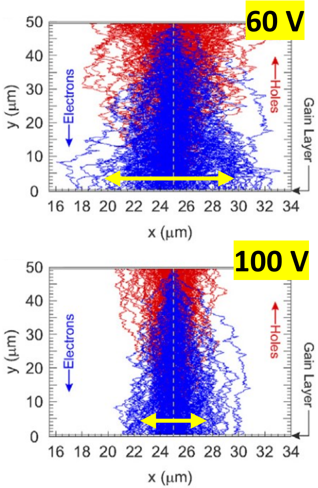

Increased electric field **screening** at higher bias due to the faster drift and smaller lateral spread of the charge cloud (diffusion)

2) Changing angle of incidence

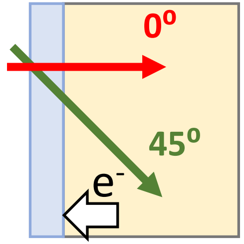

Perpendicular and 45° angle protons with ≈ ion. profile -> quantify gain

Results confirm **crucial influence** of the radiation *ionization density*

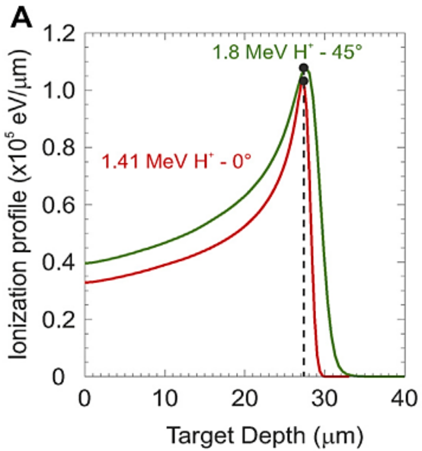

MIP-like behavior for angled ionization

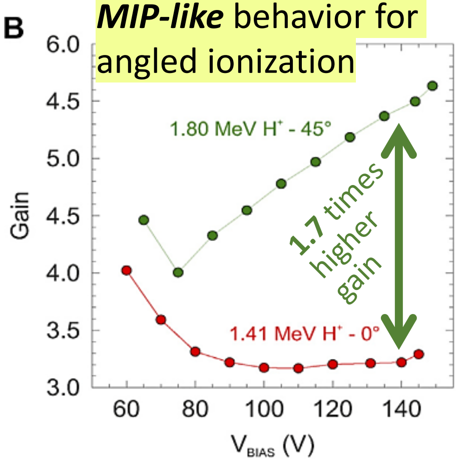

Gain suppression in Low Gain Avalanche Diodes (LGAD)

1) Different penetration depths

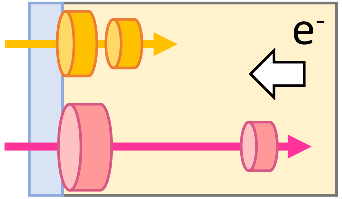

G. Kramberger – KDetSim code

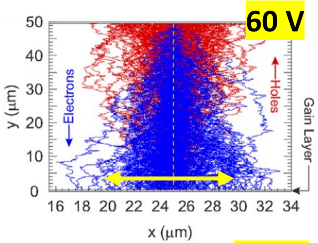

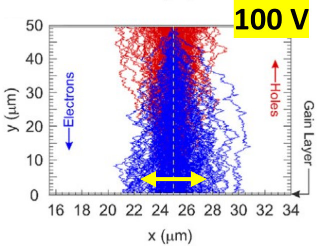

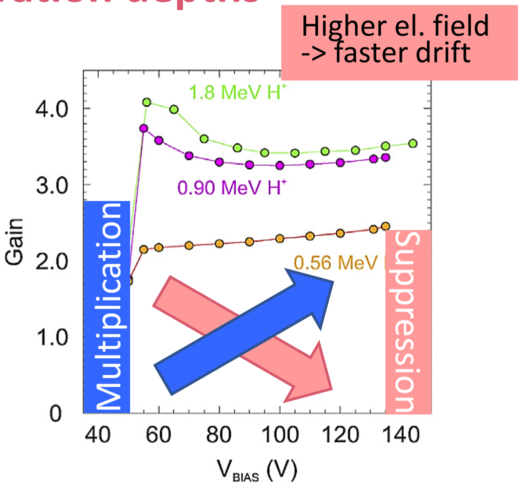

Increased electric field **screening** at higher bias due to the faster drift and smaller lateral spread of the charge cloud (diffusion)

2) Changing angle of incidence

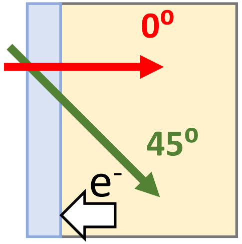

Perpendicular and 45° angle protons with ≈ ion. profile -> quantify gain

Results confirm **crucial influence** of the radiation *ionization density*

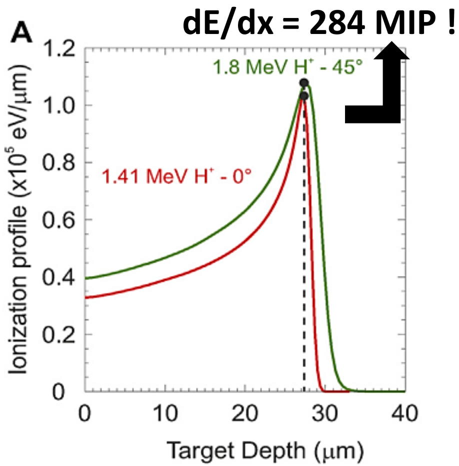

MIP-like behavior for angled ionization

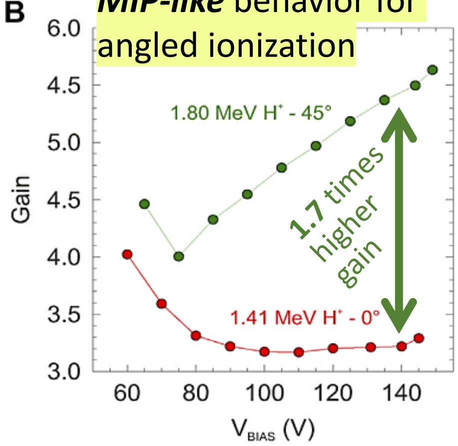

Please see previous reports from the Seville group:

Sebastian Pape - 40th meeting

Maria Del Carmen Jimenez Ramos – 38th meeting

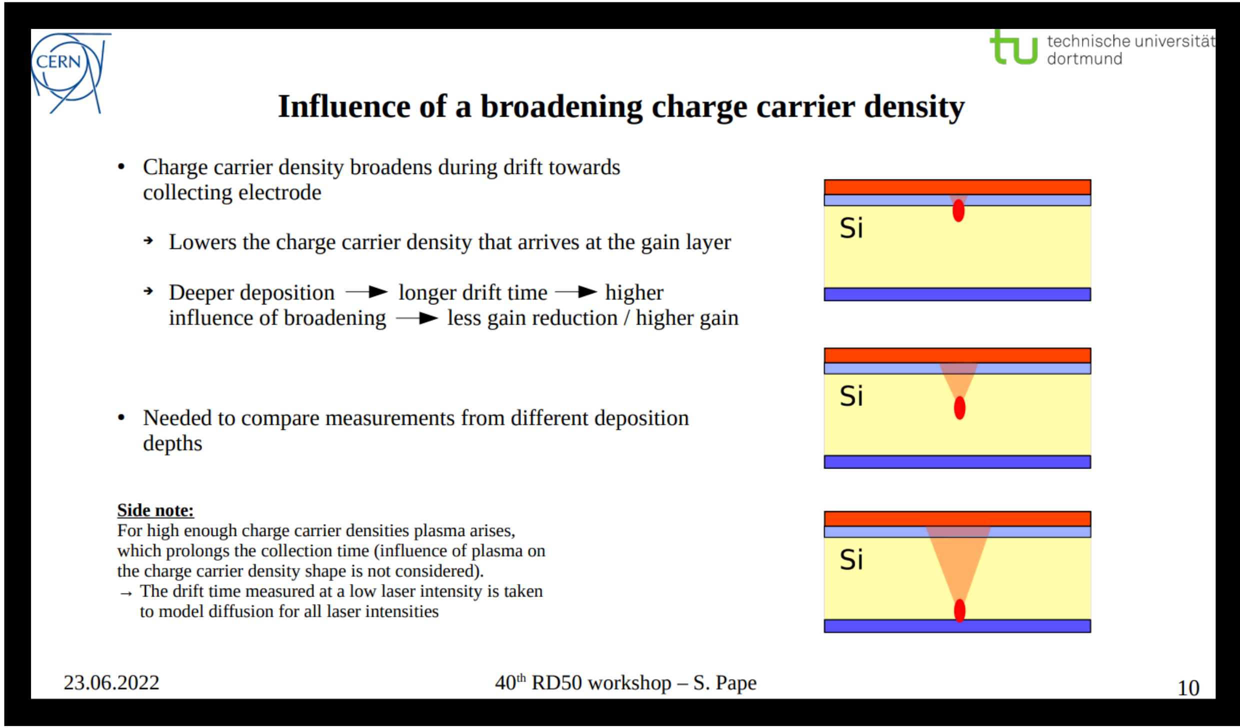

Gain suppression when the Bragg peak is in the active volumen

1) Between 70° and 85° the number of the electrons created closer to the anode becomes larger.
The multiplication factor grows exponentially with the distance travelled by the electrons within the multiplication layer.

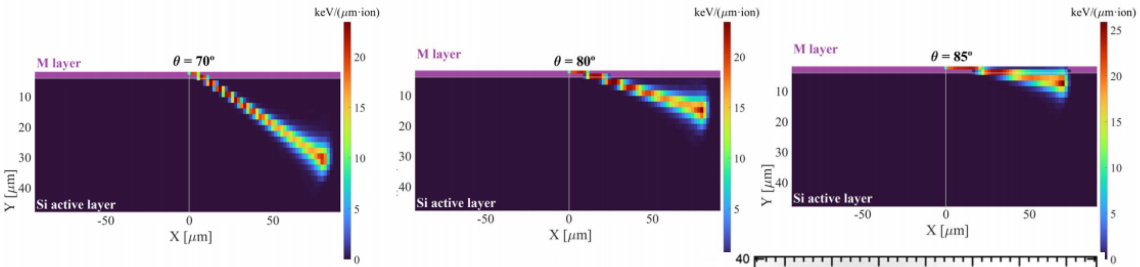

2) Due to ambipolar diffusion, the closer the Bragg peak is deposited to the gain layer, the higher the ionization density because the carriers have less time to diffuse in the direction perpendicular to the electric field.

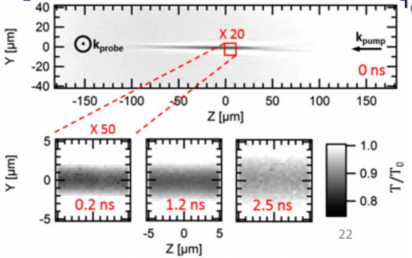

Appl. Phys. Lett. 108, 041107 (2016)
FIG. Direct observation of free-carrier diffusion inside silicon. A microplasma induced by two-photon ionization with a focused femtosecond laser pulse. High-resolution images acquired for different delays between pump and probe (bottom images) reveal directly the expansion of the microplasma by free-carrier diffusion.

Please see previous reports from the Seville group:

Sebastian Pape - 40th meeting

Maria Del Carmen Jimenez Ramos – 38th meeting

technische universität dortmund

dening charge carrier density

towards

ves at the gain layer

→ higher

duction / higher gain

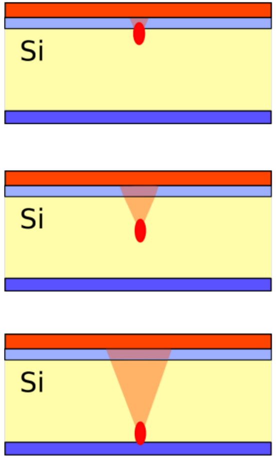

- Needed to compare measurements from different deposition depths

Side note:
For high enough charge carrier densities plasma arises, which prolongs the collection time (influence of plasma on the charge carrier density shape is not considered).
→ The drift time measured at a low laser intensity is taken to model diffusion for all laser intensities

23.06.2022 40th RD50 workshop – S. Pape 10

Additional examples

Analysis of Ion – TCT signals

Carbon ions of different energy (injected from the top electrode)

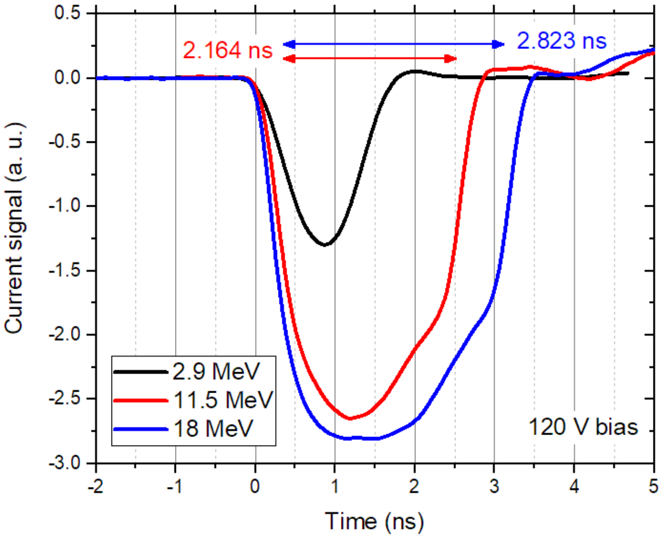

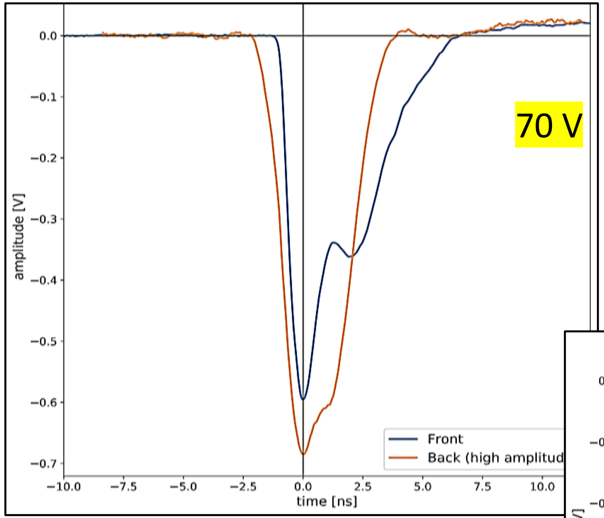

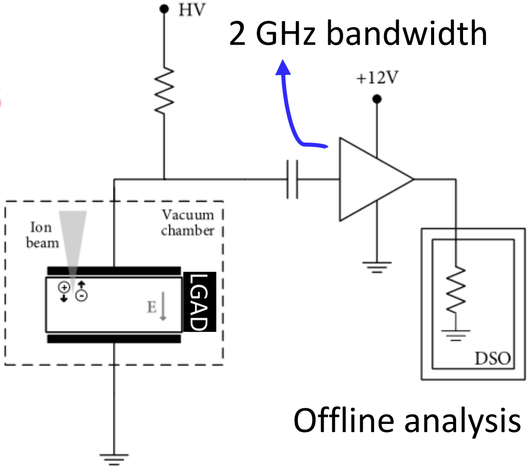

Offline analysis

4 MeV protons, injected from the top or the back electrode

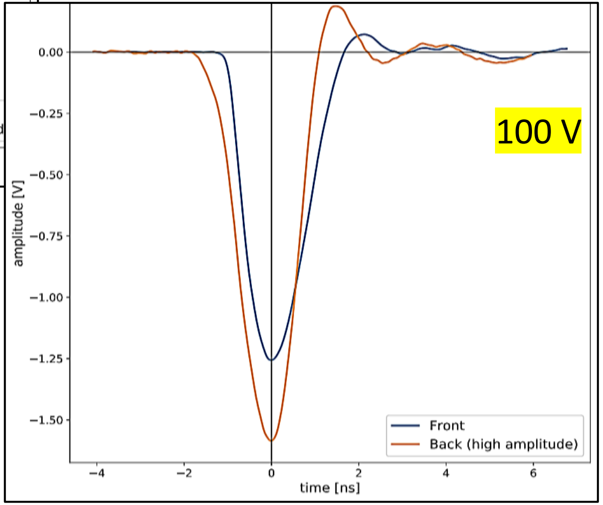

Additional examples

Radiation damage studies with μBeam

Additional examples

Radiation damage studies with µBeam

Comparison of pristine and proton damaged diamond detector charge transient signals

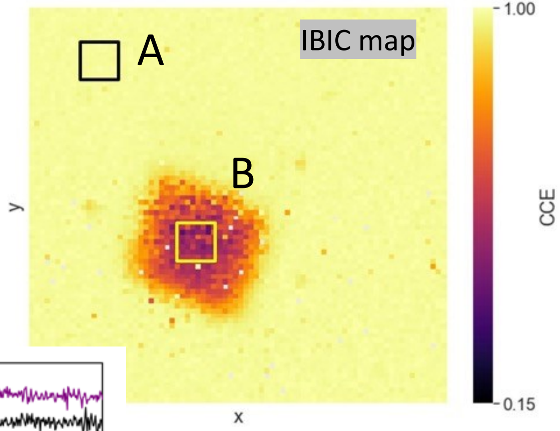

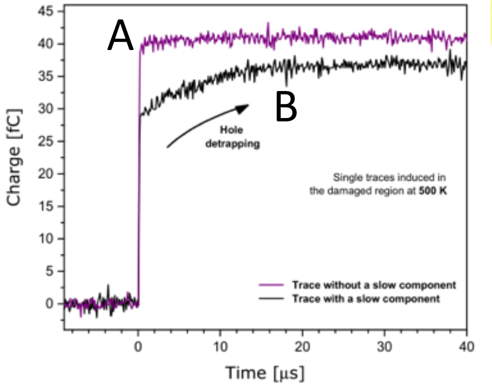

$$\tau_D^{-1} = \sigma \Gamma T^2 \exp(-E_a/k_B T)$$

Additional examples

Radiation damage studies with μBeam

Comparison of pristine and proton damaged diamond detector charge transient signals

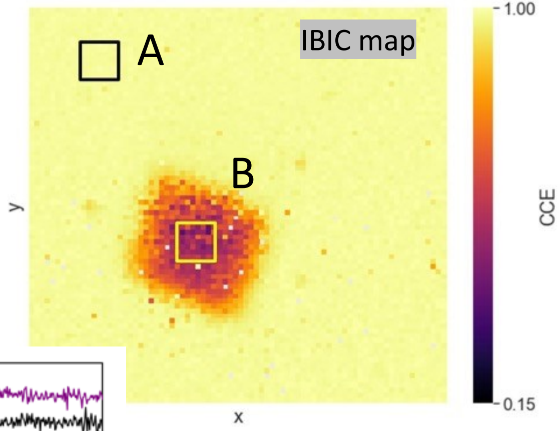

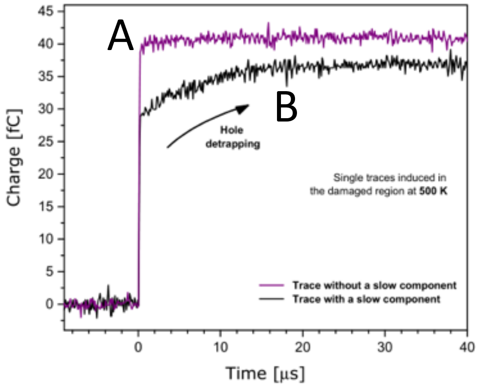

$$\tau_D^{-1} = \sigma \Gamma T^2 \exp(-E_a/k_B T)$$

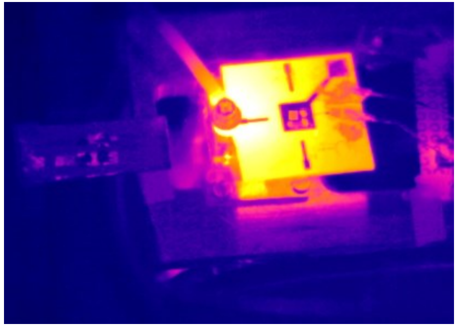

Additional examples

Radiation damage studies with µBeam

Comparison of pristine and proton damaged diamond detector charge transient signals

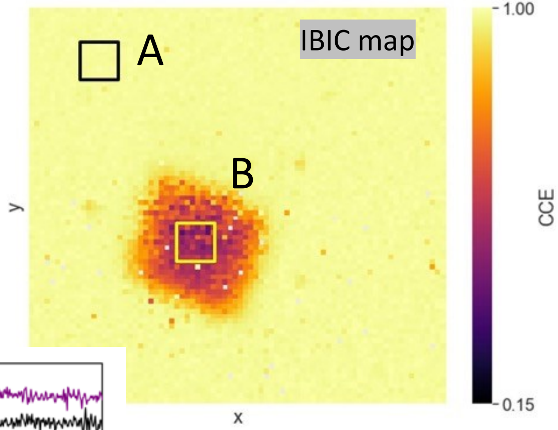

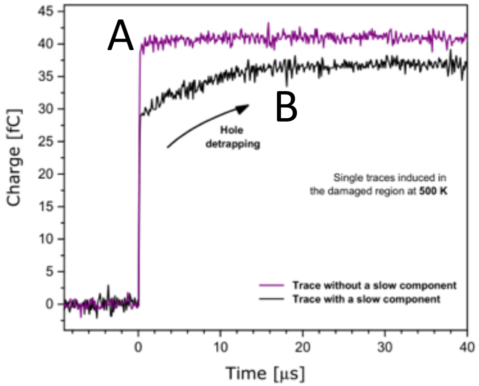

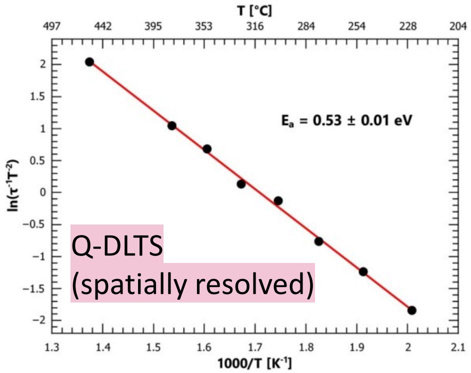

$$\tau_D^{-1} = \sigma \Gamma T^2 \exp(-E_a/k_B T)$$

Additional examples

Radiation damage studies with µBeam

Comparison of pristine and proton damaged diamond detector charge transient signals

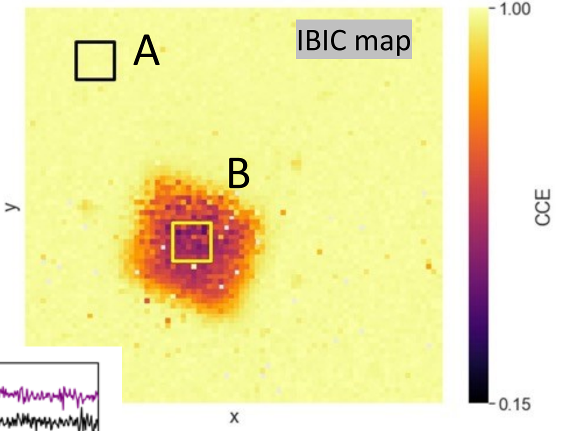

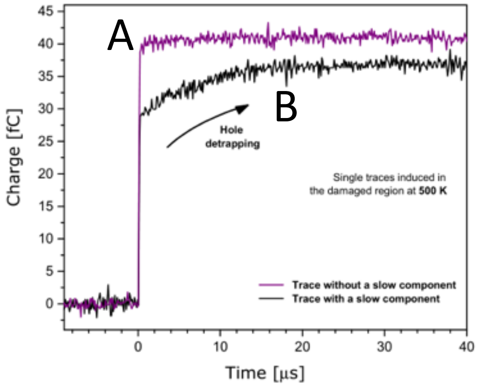

$$\tau_D^{-1} = \sigma \Gamma T^2 \exp(-E_a/k_B T)$$

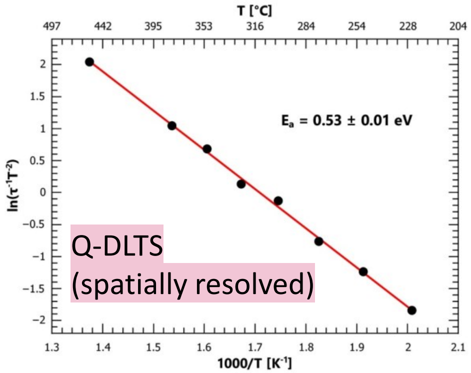

AIDA innova

Sample heating and cooling (40 K – 1000 K)

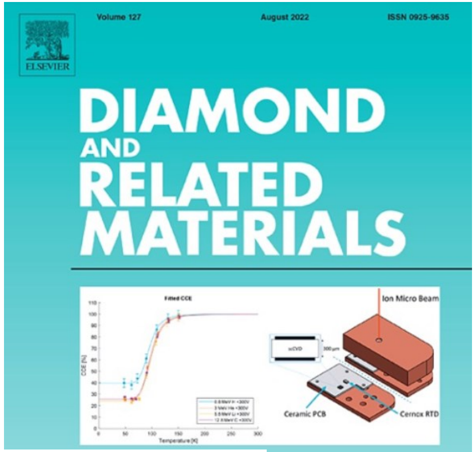

Charge collection efficiency of scCVD diamond detectors at low temperatures

D. Cosic[a,*], G. Provatas[a], M. Jakšić[a], D. Begušić[b]

[a] Ruđer Bošković Institute, Zagreb, Croatia
[b] Faculty of Electrical Engineering, Mechanical Engineering and Naval Architecture, University of Split, Split, Croatia

materialstoday Connecting the materials community

Additional examples

Radiation damage studies with µBeam

Comparison of pristine and proton damaged diamond detector charge transient signals

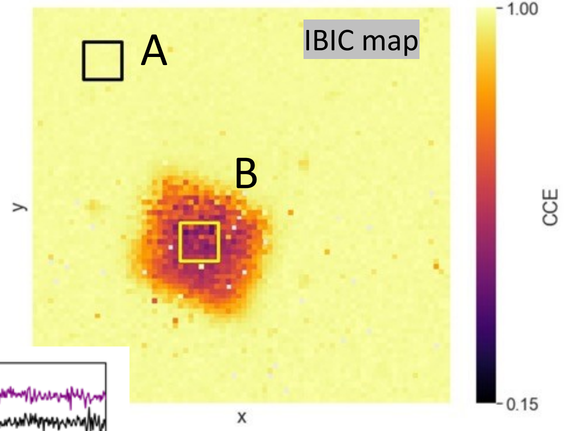

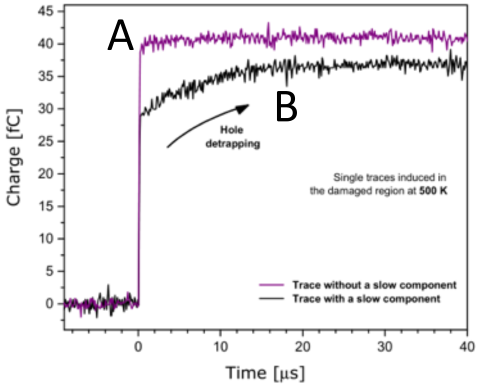

$$\tau_D^{-1} = \sigma \Gamma T^2 \exp(-E_a/k_B T)$$

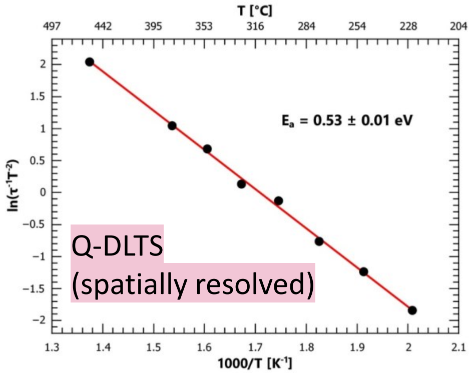

ON-LINE monitoring of induced damage

- Direct (IBIC)
- Indirect (chopping + RBS)

Additional examples

Radiation damage
studies with µBeam

Comparison of pristine and proton damaged diamond detector charge transient signals

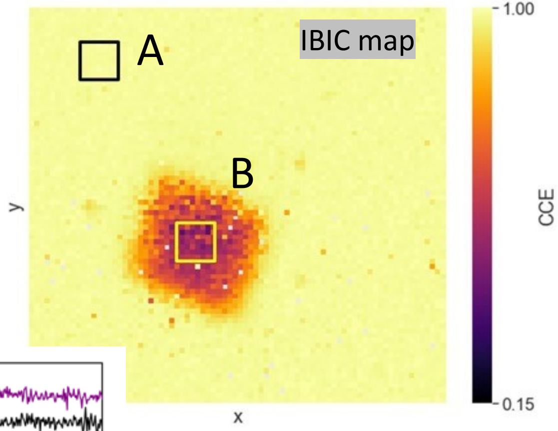

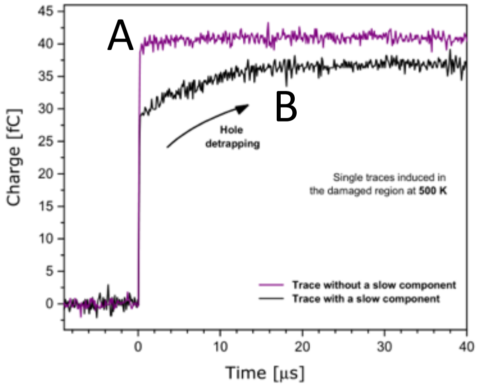

$$\tau_D^{-1} = \sigma \Gamma T^2 \exp(-E_a/k_B T)$$

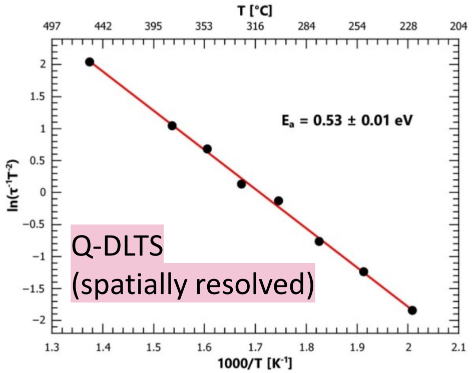

ON-LINE monitoring of induced damage

- Direct (IBIC)
- Indirect (chopping + RBS)

< 5% fluence error

Additional examples

Radiation damage studies with µBeam

Comparison of pristine and proton damaged diamond detector charge transient signals

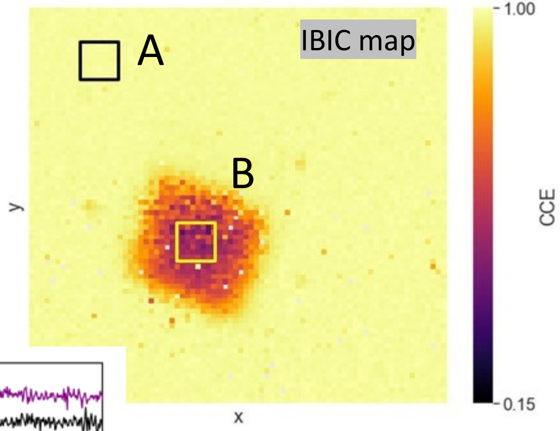

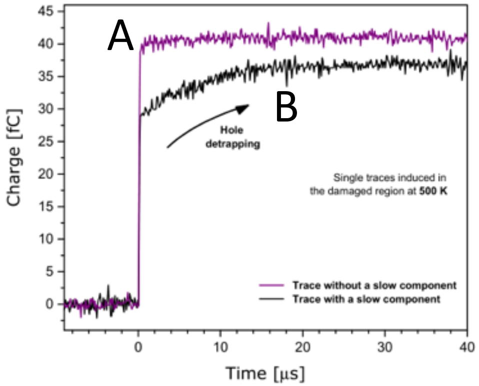

$$\tau_D^{-1} = \sigma \Gamma T^2 \exp(-E_a/k_B T)$$

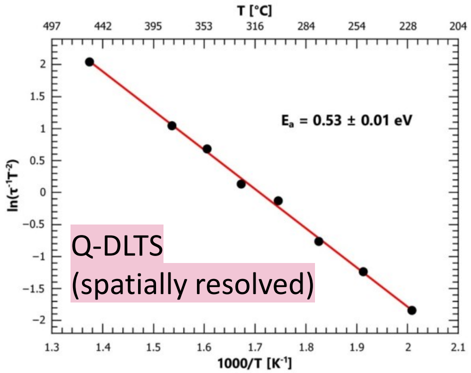

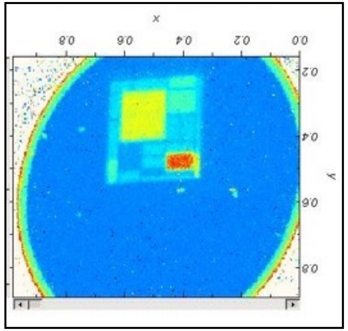

ON-LINE monitoring of induced damage

- Direct (IBIC)
- Indirect (chopping + RBS)

< 5% fluence error

Additional examples

Radiation damage studies with μBeam

Comparison of pristine and proton damaged diamond detector charge transient signals

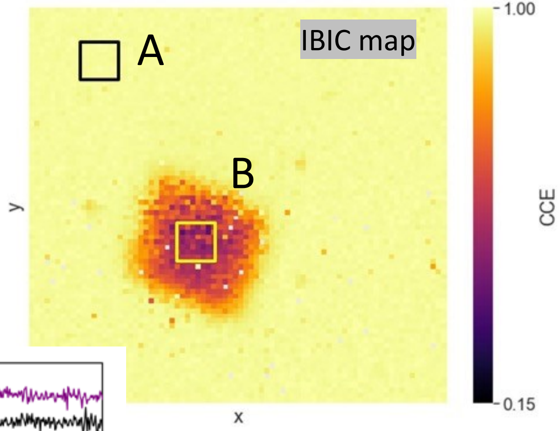

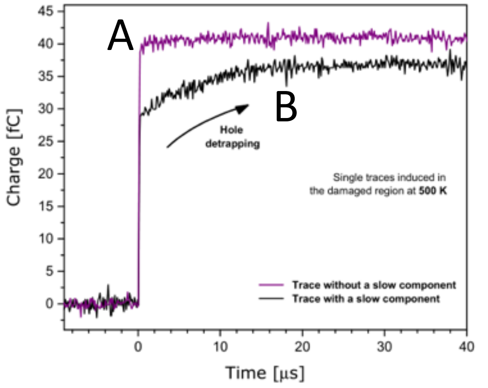

$$\tau_D^{-1} = \sigma \Gamma T^2 \exp(-E_a/k_B T)$$

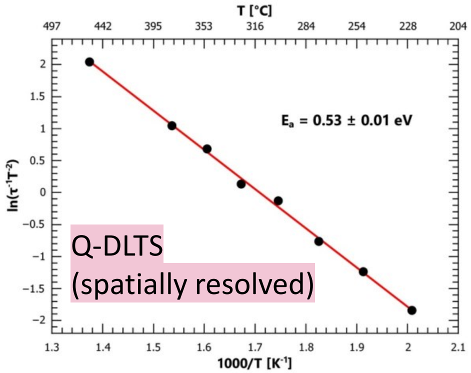

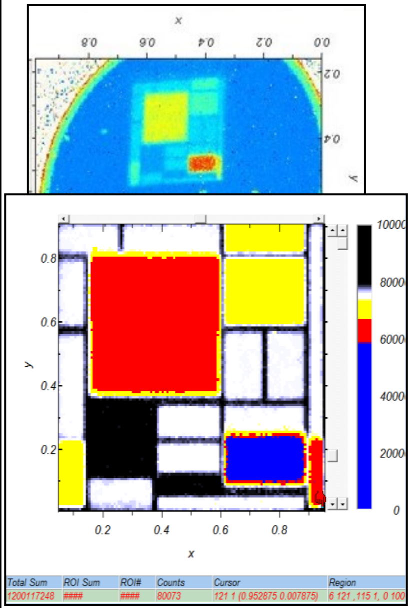

ON-LINE monitoring of induced damage

- Direct (IBIC)
- Indirect (chopping + RBS)

< 5% fluence error

Additional examples

Radiation damage studies with μBeam

Comparison of pristine and proton damaged diamond detector charge transient signals

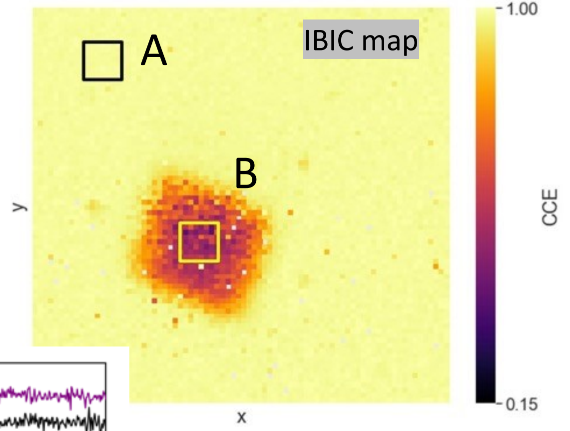

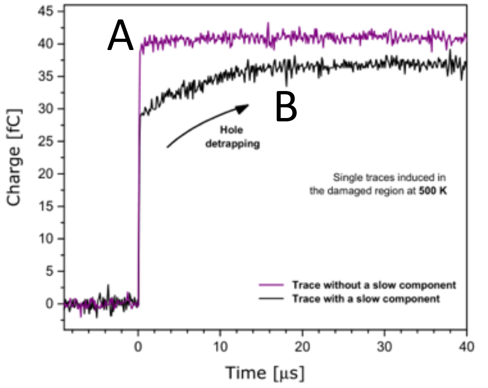

$$\tau_D^{-1} = \sigma \Gamma T^2 \exp(-E_a/k_B T)$$

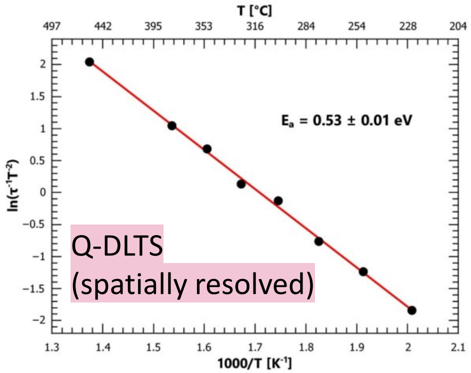

ON-LINE monitoring of induced damage

-
-

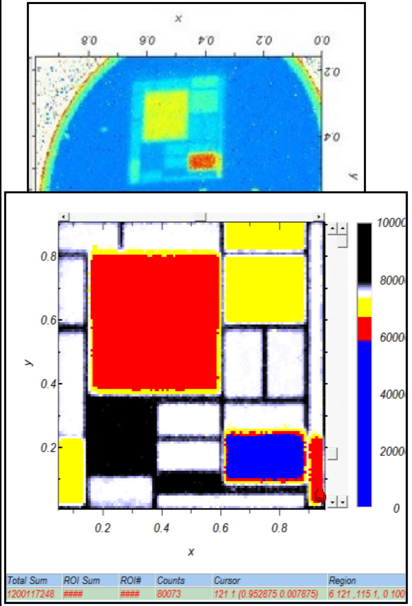

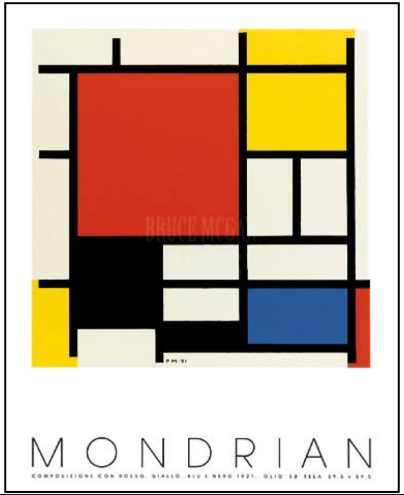

Summary

- MeV ions injected in LGAD samples to induce high ionization and study gain suppression physics
- Deeply penetrating protons experience lower gain suppression with increasing electric field as compared to shallow penetrating protons – diffusion of the charge cloud
- Probing with frontal and 45° ion beam with similar ionization profile demonstrates critical influence of ionization density on gain performance
- Ion-TCT signals induced by ions injected from the top and the back side – shape analysis
- Additional ion microprobe capabilities:
  - Selective introduction of the radiation damage
  - Online monitoring of the accumulated fluence

REFERENCES:

[1] Curras E, et al.. Gain Suppression Mechanism Observed in Low Gain Avalanche Detectors. Nucl Instr Meth(2022) A1031:166530.

[2] Jiménez-Ramos, M.C., et al. Study of Ionization Charge Density-Induced Gain Suppression in LGADs. Sensors 2022, 22, 1080.

[3] Jakšić M. et al. Ion Microbeam Studies of Charge Transport in Semiconductor radiation Detectors With Three-Dimensional Structures: An Example of LGAD. Front. Phys. (2022) 10:877577.

FUNDING

Center of Excellence for Advanced Materials and Sensing Devices

IAEA International Atomic Energy Agency

Additional support:
H2020 Research and Innovation programme (Grant No. 101004761)
Slovenian Research Agency project (J1 – 1699)

Trans-national access to RBI facility

Collaborations from the last 6 years regarding detector testing
Through the AIDA2020 and RADIATE (more than 20 experiments)

- **AIDA-2015-1**, Study of radiation damage in scCVD diamond, Jerzy Pietraszko, GSI, **Germany (26-30.10.2015.)**
- **AIDA-2015-2**, Diamond Membranes for Radioisotope Batteries, Michal Pomorski, CEA, **France (15-19.2.2016.)**
- **AIDA-2015-4**, 3D diamond, Alexander Oh, University of Manchester, **UK (11-15.4.2016.)**
- **AIDA-2016-1**, Single crystal diamond Shottky diodes for microdosimetry, Claudio Verona, **Italy (24-28.10.2016).**
- **AIDA-2016-2**, Microbeam tests of silicon telescope for dosimetry, G. Magrin, **Austria (18-20.1. and 9-10.2.2017.)**
- **AIDA-2017-1:** Diamond Membrane Microdosimeter, M. Pomorski, CEA, **France (2-5.5.2017.)**
- **AIDA-2017-4:** CVD diamond Time of Flight detector with interdigitated electrodes, W. Cayzac, **France (6-10.11.2017)**
- **AIDA-2017-5:** Polycrystalline 3D Diamond IBIC and TRIBIC characterisation, A. Oh, Manchester, **UK (27.11.-2.12.2017).**
- **AIDA-2017-2:** Analysis of graphite pillars buried in sc-CVD diamond , G. Conte, **Italy (12-14.9.2017. and 20-21.3.2018)**
- **AIDA-2018-1:** Single event upsets in CMS pixel ROC, Wolfram Erdmann, PSI **Switzerland (2.7.-6.7.2018).**
- **AIDA-2019-1:** IBIC of monolytic pixel detectors, Rogelio Pinto, University of Sevilla, **Spain (19.8.-23.8.2019).**

1. **E. Vittone, Italy,** Differential IBIC analysis for the measurement of carrier lifetime in silicon pin diodes **(20.-22.5.2020)**
2. **M. Pomorski, France,** 3D scCVD diamond membrane microdosimeter for quality assurance in hadron therapy **(24.-27.8.2020)**
3. **A. Oh, UK,** Charge collection of 3D diamond and LGAD test detectors with the proton microbeam **(7.-11.6.2021)**
4. **R. Pinto, Spain,** Response in monolithic particle detector for the RD50 collaboration **(14.-18.6.2021)**
5. **C. Verona, Italy,** Characterization of ΔE-E single crystal diamond based telescope for microdosimetry application **(5.-9.7.2021)**
6. **E. Vittone, Italy,** Hydrogen thermal donors in silicon **(22.-24.2.2022)**
7. **C. Verona, Italy,** IBIC characterization of single crystal diamond devices for microdosimetry application **(7.-11.2.2022)**
8. **A. Oh, UK,** Investigation of charge collection of hexagonal and cubic 3D diamond detectors **(4. – 8.4.2022.)**
9. **M. Camarada, Switzerland,** Study of charge transport response of Silicon Carbide sensors **(2.-6.5.2022.)**
10. **M. Camarada, Switzerland,** Study of high temperature charge transport response of SiC **(planned for 19.-23.9.2022)**

New applications – EuroLABS (2022 – 2026)

This proposal brings together for the first time in Europe the three communities engaged in Nuclear Physics and Accelerator/ Detector technology for High Energy Physics.

https://web.infn.it/EURO-LABS/wp4/

Type of facility	Access provider	Infrastructure	Country	Facility Coordinator Contact
Beam test	CERN	PS & SPS	International Organization	Barbara Holzer
	DESY	DESY-II	Germany	Marcel Stanitzki
	PSI	PiM1	UCN	Tilman Rohe
Detector characterization	RBI	RBI-AF	Croatia	Stjepko Fazinić
	ITAINNOVA	EMClab	Spain	Fernando Arteche
Irradiations	CERN	IRRAD	International Organization	Federico Ravotti
	CERN	GIF++	International Organisation	Michael Moll
	JSI	TRIGA Reactor	Slovenia	Igor Mandic
	IFJ PAN	AIC-144	Poland	Pawel Olko
	UCLouvain	CRC	Belgium	Eduardo Cortina Gil
	UoB	MC40 Cyclotron	UK	Laura Gonella

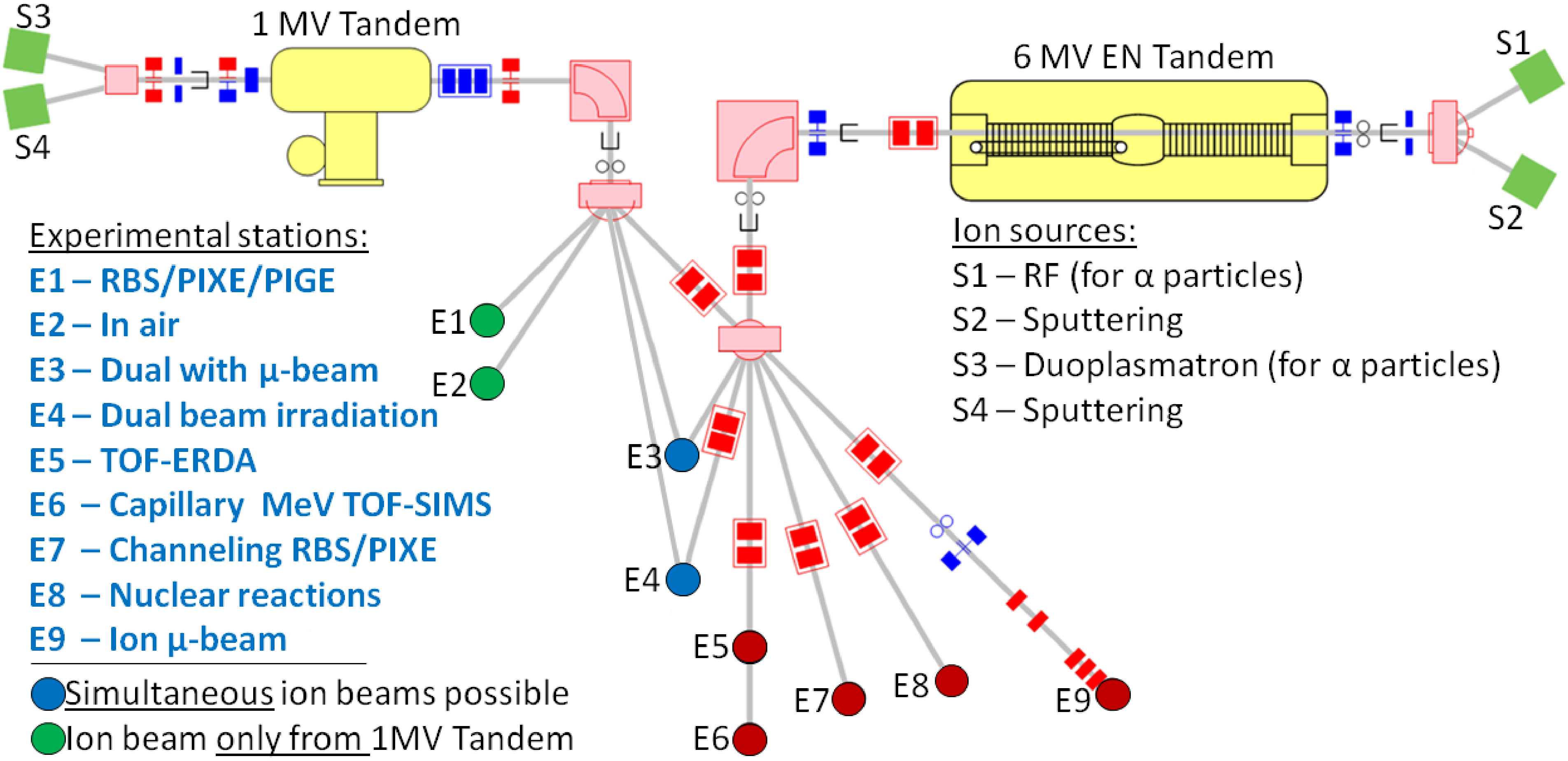

Experimental stations:

E1 – RBS/PIXE/PIGE
E2 – In air
E3 – Dual with μ-beam
E4 – Dual beam irradiation
E5 – TOF-ERDA
E6 – Capillary MeV TOF-SIMS
E7 – Channeling RBS/PIXE
E8 – Nuclear reactions
E9 – Ion μ-beam

- (blue) Simultaneous ion beams possible
- (green) Ion beam only from 1MV Tandem
- (red) Ion beam from 1MV or EN Tandem

Ion sources:

S1 – RF (for α particles)
S2 – Sputtering
S3 – Duoplasmatron (for α particles)
S4 – Sputtering